Thermal properties of $Cd_2Re_2O_7$ and $Cd_2Nb_2O_7$ at the structural phase transitions

Makoto Tachibana,[1] Naoya Taira,[2] Hitoshi Kawaji,[2] and Eiji Takayama-Muromachi[1]
[1]*National Institute for Materials Science, Namiki 1-1, Tsukuba, Ibaraki 305-0044, Japan*
[2]*Materials and Structures Laboratory, Tokyo Institute of Technology, 4259 Nagatsuta-cho, Midori-ku, Yokohama 226-8503, Japan*
(Received 27 May 2010; published 13 August 2010)

The structural phase transitions in $Cd_2Re_2O_7$ and $Cd_2Nb_2O_7$ pyrochlores have been studied through capacitive thermal expansion, heat capacity, and thermal conductivity. The superconductor $Cd_2Re_2O_7$ (T_c=1 K) shows well-defined anomalies at 200 and 120 K due to structural transitions. The pressure dependence of the transition temperatures is calculated from the thermal expansion and heat capacity, which shows good agreement with the results of direct measurements. The ferroelectric $Cd_2Nb_2O_7$ shows distinct anomalies due to structural transitions at 204, 85, and 46 K, in addition to a broad feature around 190 K associated with the relaxorlike behavior. For both compounds, the lattice thermal conductivity shows a glasslike temperature dependence in the high-temperature cubic phase.

DOI: 10.1103/PhysRevB.82.054108 PACS number(s): 74.70.−b, 77.84.Ek, 65.40.−b, 77.80.B−

I. INTRODUCTION

Pyrochlore oxides with the general formula $A_2B_2O_7$ exhibit a wide range of complex phenomena, including colossal magnetoresistance, metal-insulator transition, and geometrical frustration of magnetic spins.[1,2] The cubic pyrochlore structure (space group $Fd\bar{3}m$) consists of a three-dimensional network of corner-sharing BO_6 octahedra, which has the composition $(B_2O_6)_\infty$. This leaves the A metals and the seventh set of oxygen ions, denoted as O′, to occupy the open spaces and form a network of A_2O' sublattice. The presence of two interpenetrating networks lead to important properties, that are not observed in otherwise related systems such as the ABO_3 perovskites: a notable example is the separation of magnetic and transport channels in the magnetoresistive $Tl_2Mn_2O_7$.[3]

Interestingly, only very few pyrochlores display structural phase transition,[1,2] which is in contrast to many examples found in perovskites. Among these, the pyrochlore superconductor[4] $Cd_2Re_2O_7$ (with a superconducting T_c =1 K) attracted particular recent interest. $Cd_2Re_2O_7$, which is cubic at room temperature, undergoes a second-order transition to a tetragonal $I\bar{4}m2$ phase at T_{R1}=200 K and a first-order transition to a tetragonal $I4_122$ phase at T_{R2}=120 K.[5] Both tetragonal structures are noncentrosymmetric. Sergienko *et al.*[6,7] established that the 200 K transition is driven by the softening of a zone center, twofold-degenerate E_u optic mode, which corresponds to a ferrodistortive displacement of the ReO_6 octahedra. Therefore, $Cd_2Re_2O_7$ may be regarded as a rare example of "ferroelectric" metal.[7,8] Subsequent discovery of Goldstone optic-phonon excitations,[9,10] which arise from long-wavelength fluctuations between the nearly degenerate $I\bar{4}m2$ and $I4_122$ structures, fueled additional excitement on this compound. On the other hand, there is currently little understanding on the second transition at T_{R2}, as it is accompanied by very weak anomalies in the structure and physical properties.[5,11] Resistivity[12,13] and thermopower[13] measurements under pressure showed that both T_{R1} and T_{R2} decrease with increasing pressure, with the superconductivity disappearing before the cubic phase is stabilized down to the lowest temperature.[12]

$Cd_2Nb_2O_7$ is another pyrochlore compound that displays a sequence of structural phase transitions. Below room temperature, this cubic insulator first undergoes a second-order transition to an orthorhombic phase at $T_{N1}\approx 205$ K, which is often described as improper ferroelastic.[14] Around 190 K, $Cd_2Nb_2O_7$ shows a broad peak in heat capacity[15] and a frequency-dependent relaxation peak in dielectric susceptibility,[14,15] which are reminiscent of ferroelectric relaxors.[16] However, $Cd_2Nb_2O_7$ lacks the compositional disorder found in conventional relaxors [e.g., $Pb(Mg_{1/3}Nb_{2/3})O_3$] and the origin of the relaxorlike behavior is not well understood. Furthermore, there is no clear connection between the relaxorlike behavior and the ferroelectric soft mode,[14,17] the latter apparently showing a phase transition at $T_{N2}\approx 196$ K. Below this temperature region, the reported space group is orthorhombic $Ima2$.[18] Symmetry analysis[14] and first-principles calculations[19] identified the threefold degenerate T_{1u} mode as the ferroelectric soft mode with the Nb ions showing predominant displacement.[19] At much lower temperatures, $Cd_2Nb_2O_7$ shows a second-order transition at T_{N3}=85 K and a first-order transition at T_{N4} =46 K.[15] From Raman-scattering[20,21] and heat-capacity[15] measurements, an incommensurate phase for the temperatures between T_{N3} and T_{N4} has been suggested. However, the x-ray diffraction study[18] only reported an average symmetry of monoclinic Cc below T_{N3} with no evidence of satellite peaks expected for an incommensurate structure.[22]

Although $Cd_2Re_2O_7$ and $Cd_2Nb_2O_7$ have been studied separately for the most part, the following observations suggest that there may be important connections between the two compounds: (1) among the hundreds of known pyrochlore compounds,[1,2] $Cd_2Re_2O_7$ and $Cd_2Nb_2O_7$ are the two rare examples showing displacive (soft-mode driven) structural transitions.[23] This is particularly remarkable, as structural instability is generally governed by a delicate balance between Coulomb and repulsive ionic interactions,[25,26] and these interactions are expected to be very different between metallic and insulating compounds. (2) For both compounds, dynamic or static disorder of Cd ions has been invoked to explain specific features of the transitions. For $Cd_2Re_2O_7$, a Raman-scattering study[27] found additional phonon modes below T_{R2}, which were linked to ordering of the Cd ions.

Additionally, a recent study[28] found glasslike behavior in the lattice thermal conductivity, which was ascribed to the interaction between the heat-carrying acoustic phonons and the localized Einstein oscillation of the Cd ions. In $Cd_2Nb_2O_7$, the overdamped character of the ferroelectric soft mode was explained by the coupling of the soft mode to the dynamic disorder of the Cd ions,[14,17] and the relaxorlike behavior has been associated with the reorientation of Cd-O′ dipole chains.[29,30] Recently, a diffuse x-ray scattering study[31] found strong evidence for the dynamical off-center displacement of the Cd ions in the cubic phase. (3) Both compounds show successive structural transitions, with only the lowest-temperature one being first order in both cases. The interplay of the rigid ReO_6/NbO_6 network and the flexible Cd_2O' chains may be important in understanding the sequence of structural transitions.

In an effort to improve the understanding of the structural transitions, this study focuses on the thermal expansion, heat capacity, and thermal conductivity of $Cd_2Re_2O_7$ and $Cd_2Nb_2O_7$ single crystals. The combination of heat capacity and thermal expansion provides the initial pressure dependence of the transition temperatures, which can be compared with the results of direct measurements. Thermal conductivity is sensitive to anharmonic interactions and local lattice distortions,[32] which makes it a valuable probe to study the change in lattice dynamics across the transitions. For both compounds, we discuss the anomalous features of the thermal properties that provide insights on the nature of the structural transitions.

II. EXPERIMENT

For this study, single crystals of $Cd_2Re_2O_7$ were grown by the vapor transport method. Stoichiometric mixtures of CdO, Re, and ReO_3 were sealed in an evacuated quartz tube and heated at 1223 K for six days. The phase purity of the crystals was checked with powder x-ray diffraction. Resistivity was measured by a four-probe dc method and magnetic susceptibility was obtained with a commercial magnetometer under a magnetic field of 10 kOe. Heat capacity was measured by the relaxation technique using a Quantum Design physical properties measurement system (PPMS). The same crystal was used for these measurements and the thermal-expansion measurements described below.

The single crystals of $Cd_2Nb_2O_7$ came from the same batch used in Ref. 15, which were grown by the flux method using CdO and B_2O_3 as the flux. The heat capacity of $Cd_2Nb_2O_7$ obtained with the relaxation technique showed excellent agreement with Ref. 15, in which the data were obtained with an adiabatic calorimeter on a collection of single crystals. Because the adiabatic technique has higher accuracy and precision, we reproduce the heat capacity data reported in Ref. 15.

Thermal-expansion measurements on $Cd_2Re_2O_7$ and $Cd_2Nb_2O_7$ were carried out with a capacitance dilatometer, which is made of silver and described in Ref. 33. To perform measurements along the cubic ⟨111⟩ direction, the crystals were oriented with a Laue camera and parallel surfaces were prepared by polishing. The distance between the two surfaces was 3.26 nm and 1.84 mm for $Cd_2Re_2O_7$ and $Cd_2Nb_2O_7$, respectively. It should be noted that thermal expansion along the cubic ⟨111⟩ is not affected by the distribution of tetragonal domains below the transition.[34] The linear thermal expansivity $\Delta L/L_0$ ($\Delta L = L - L_0$ and L_0 refers to the value at 293 K) was obtained while continuously heating the crystal with a rate of 1 K/min between 2 and 300 K. Measurements were repeated with different mountings and reproducibility was checked. Also, measurements on a reference copper sample showed that the accuracy is better than 1%. To calculate the thermal-expansion coefficient $\alpha = d(\ln L)/dT$, we averaged several consecutive points of the $\Delta L/L_0$ data with a Gaussian weighting around each temperature, which was then differentiated. We checked the validity of the averaging by comparing the results with those of point-by-point differentiation. Especially, we confirmed that the sharp features of the transitions are fully retained through the averaging but with reduced scatter. Thermal-conductivity measurements on irregularly shaped crystals, with the longest dimension of ~5 mm, were performed with the PPMS using the thermal transport option. This apparatus uses a radiation shield to minimize heat loss via radiation, and the remaining heat loss is estimated from the emissivity and surface area of the sample using the measurement program. This correction is typically ~10–20 % at 300 K and negligible below 100 K. Due to uncertainties in the cross sections of the crystals, the absolute accuracy of the data is estimated to be ~20%.

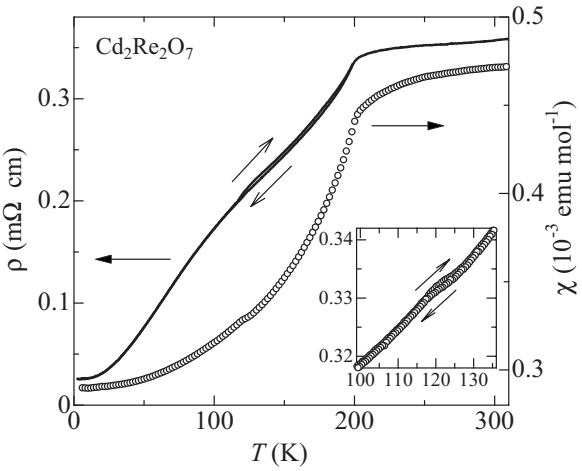

FIG. 1. Resistivity ρ and magnetic susceptibility χ of $Cd_2Re_2O_7$. χ was measured under a magnetic field of 10 kOe. The inset shows χ in the vicinity of the 120 K transition.

III. RESULTS AND DISCUSSION

A. Heat capacity and thermal expansion of $Cd_2Re_2O_7$

We first focus on the thermodynamic properties of $Cd_2Re_2O_7$. Figure 1 presents the resistivity ρ and magnetic susceptibility χ of the $Cd_2Re_2O_7$ crystal, which show good overall agreement with the previous studies.[11,35] The most prominent feature is the sharp drop in ρ and χ at $T_{R1} = 200$ K, which signifies a large modification of the Fermi

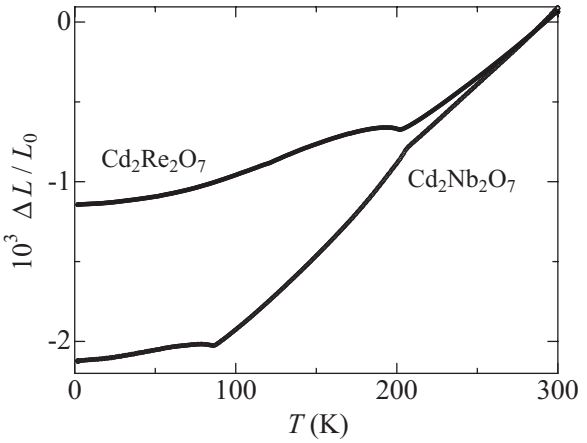

FIG. 2. The temperature dependence of the linear thermal expansivity $\Delta L/L_0$ of $Cd_2Re_2O_7$ and $Cd_2Nb_2O_7$ along the cubic ⟨111⟩ direction.

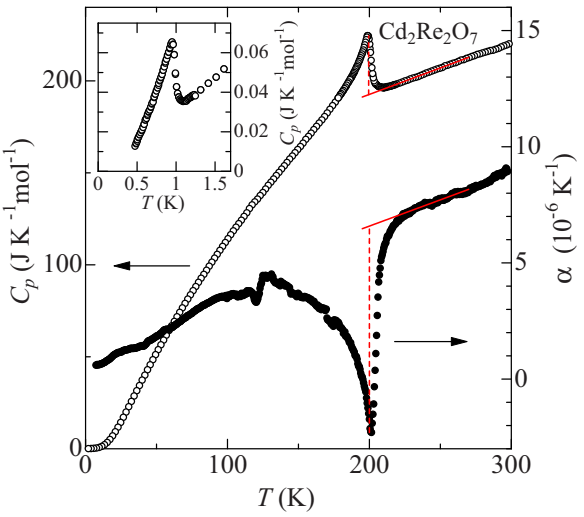

FIG. 3. (Color online) Heat capacity C_p and thermal-expansion coefficient α of $Cd_2Re_2O_7$. The lines are extrapolations from the high-temperature cubic phase, which are used to obtain the jumps in C_p and α at $T_{R1}=200$ K (dashed lines). The inset shows C_p in the vicinity of the superconducting transition at 1 K.

surface at this structural transition.[28,35] There is a weaker anomaly at $T_{R2}=120$ K, where the hysteresis between the heating and cooling directions (χ near T_{R2} is shown in the inset) confirms the first-order character of the transition. While the anomaly in ρ is comparable to the previous result,[11] the anomaly in χ is much larger in this study.

The linear thermal expansivity $\Delta L/L_0$ of $Cd_2Re_2O_7$ is shown in Fig. 2. In the cubic phase above T_{R1}, the lattice contracts with decreasing temperature, in a manner consistent with the results of x-ray[36] and neutron-diffraction[37] studies. There is small expansion on cooling at T_{R1}, which is followed by normal thermal contraction down to 2 K. A much smaller anomaly can be found at T_{R2} and this will be discussed later. It should be noted that the single-crystal x-ray diffraction,[36] the powder neutron diffraction,[37] and the present capacitive measurements all give different behavior of the lattice below T_{R1}. From the tetragonal broadening of x-ray diffraction patterns, Castellan *et al.*[36] showed that the longer tetragonal axis expands continuously from T_{R1} to 15 K while the shorter axis expands from T_{R1} to ~140 K and contracts at lower temperatures. On the other hand, based on Rietveld refinement of powder neutron diffraction, Wells *et al.*[37] reported almost constant behavior for one of the tetragonal axes and slight expansion for the other axis between 150 and 13 K. Apparently, these results are in qualitative disagreement with the $\Delta L/L_0$ data along the cubic ⟨111⟩, which correspond to the weighted average of the tetragonal axes. Although we have no clear explanation for the discrepancy, it may be important to recall that the tetragonal distortion is extremely small,[36,37] which could lead to systematic errors in the structural analysis. As described below, when the present capacitive data are used to calculate the pressure dependence of the transition temperatures, good agreement with the direct results is obtained. This is strong evidence for the accuracy of the capacitive data, at least in the vicinity of the transitions.

The heat capacity C_p and thermal-expansion coefficient α of $Cd_2Re_2O_7$ are shown in Fig. 3. The superconducting transition at 1 K, which will not be discussed further, is seen as a sharp C_p peak in the inset. In agreement with the previous studies,[11,35] there is a prominent λ-type peak in C_p at T_{R1}. A similar λ-type anomaly with a negative peak is found in α. The λ-like shapes of the anomalies indicate that the transition is strongly affected by fluctuations.[35] For this second-order transition, the initial pressure dependence of the transition temperature dT_{R1}/dP can be evaluated from the C_p and α data through the Ehrenfest relation, $dT_{R1}/dP = \Delta\beta V_m T_{R1}/\Delta C_p$. Here, $V_m=8.0\times10^{-5}$ m^3 mol^{-1} is the molar volume,[36,37] $\Delta\beta=3\Delta\alpha$ is the jump in volume thermal-expansion coefficient at T_{R1}, and ΔC_p is the jump in C_p at T_{R1}.[38] Using the baselines shown in Fig. 3, we obtain $\Delta C_p = 32$ J K^{-1} mol^{-1} and $\Delta\alpha=-8.9\times10^{-6}$ K^{-1}, which lead to $dT_{R1}/dP=-13$ K/GPa. This value is in good agreement with −16 K/GPa obtained from the 0–0.6 GPa data in the resistivity measurements.[13]

The negative pressure dependence of T_{R1} is consistent with the general observation that when a structural transition is driven by the softening of a zone-center optic mode, the transition temperature decreases with pressure.[25,26] Generally, this is explained by the stronger effect of pressure on the short-range ionic repulsions compared to the long-range Coulomb interactions, where the former stabilize the undistorted cubic structure and the latter favor ferrodistortive states.[25,26] However, since this understanding comes from studies on insulating materials, its applicability to metallic systems is not clear. Nevertheless, Anderson and Blount pointed out[39] that while free electrons screen the electric field, they may not interact strongly with the zone-center ferroelectric instability. Further, the first-principles calculations[7] on $Cd_2Re_2O_7$ showed clearly that the zone-center optic mode is at the origin of the structural instability, although the roles of free electrons were not discussed explicitly. Evidently, further theoretical studies are desirable to better understand the nature of chemical bonding and lattice interactions that are responsible for the structural transitions in metallic $Cd_2Re_2O_7$.

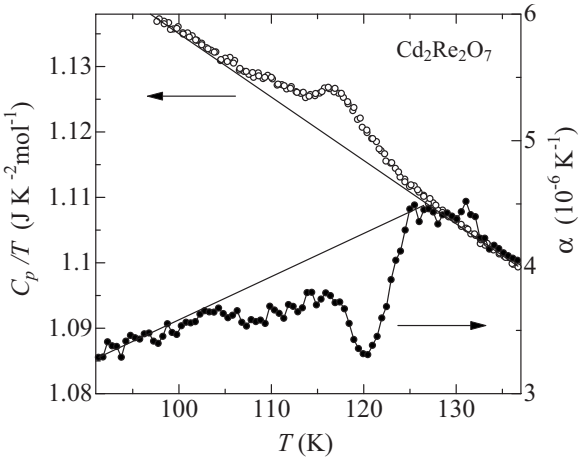

FIG. 4. Heat capacity divided by temperature, C_p/T, and thermal expansion coefficient α of $Cd_2Re_2O_7$ in the vicinity of $T_{R1}=120$ K. The lines are the baselines used to obtain the excess contributions in C_p/T and α.

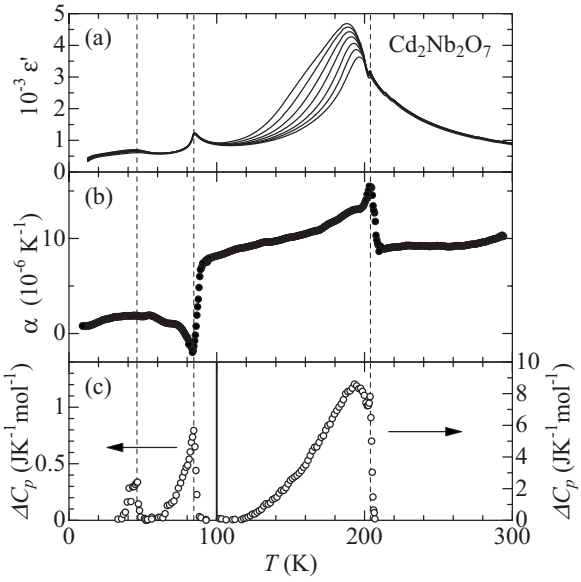

FIG. 5. (a) The real part of dielectric susceptibility ϵ' at measurement frequencies of 1, 3, 10, 30, 100, 300, and 1000 kHz (left to right), (b) the thermal-expansion coefficient α, and (c) the excess contributions to the heat capacity ΔC_p, for $Cd_2Nb_2O_7$. The data shown in (a) and (c) are reproduced from Ref. 15. Note the change in scale for ΔC_p at 100 K in (c). Dashed lines are drawn at 46, 84.5, and 204 K to locate the anomalies associated with each transition.

At the low-temperature end of the λ-type peak, another anomaly is found at T_{R2}. In Fig. 4, these anomalies are more clearly presented as plots of C_p/T and α. Here, C_p obtained on heating and cooling directions are plotted together, which show no visible difference. The size of the broad C_p/T anomaly did not change by varying the heat pulse or relaxation time of the measurement, confirming that the broadening is intrinsic to the present crystal. A similar broad anomaly is found in α, although the shape is more asymmetrical and the peak occurs at a slightly higher temperature. The broadened anomalies signify the strong sensitivity of this transition to internal inhomogeneities, such as growth strains or impurities.

For the first-order transition at T_{R2}, dT_{R2}/dP can be calculated from the Clausius-Clapyron relation $dT_{R2}/dP=\Delta V/\Delta S$, where ΔV and ΔS denote the discontinuous change in volume and entropy at T_{R2}. Here we use $\Delta V=V_m\int 3\Delta\alpha(T)dT$ and $\Delta S=\int[\Delta C_p(T)/T]dT$, which integrate the anomalous contributions. Using the baselines shown in Fig. 4, we obtain $\Delta V=-2.6\times10^{-9}$ m^3 mol^{-1} and $\Delta S=0.10$ J K^{-1} mol^{-1}, which amount to $dT_{R2}/dP=-26$ K/GPa. We find that other reasonable choices of the baselines lead to -26 ± 3 K/GPa. This dT_{R2}/dP value is to be compared with the results of thermopower measurements under pressure,[13] where an initial slope of −17 K/GPa can be identified. For that study, the largest source of error is in locating T_{R2}, especially under pressure where the anomaly becomes exceedingly small.[13] Considering the uncertainties present in both studies, the agreement in dT_{R2}/dP is deemed satisfactory. In any case, the results establish the bulk thermodynamic nature of the transition, and refute the previous suggestion[40] that the transition occurs only at the surface of the crystal.

B. Heat capacity and thermal expansion of $Cd_2Nb_2O_7$

We now turn to $Cd_2Nb_2O_7$. For this compound, $\Delta L/L_0$ in Fig. 2 shows two prominent anomalies, a change in slope at $T_{N1}=204$ K and a dip at $T_{N3}=85$ K. To examine the detailed features of each transition, we show α in Fig. 5 along with the real part of dielectric susceptibility ϵ' and the excess contributions in heat capacity ΔC_p. (The results for ϵ' and ΔC_p are reproduced from Ref. 15.) In the cubic paraelectric phase, ϵ' shows a Curie-Weiss behavior and there is no excess contributions in α and C_p. At T_{N1}, there is a sharp peak in ϵ', α, and ΔC_p, which signals the transition to the improper ferroelastic phase. If the jumps in ΔC_p and α from the high-temperature side of T_{N1} are used to calculate dT_{N1}/dP through the Ehrenfest relation, $\Delta C_p=8.0$ J K^{-1} mol^{-1}, $\Delta\alpha=6.5\times10^{-6}$ K^{-1}, and $V_m=8.4\times10^{-5}$ m^3 mol^{-1},[18] and we obtain $dT_{N1}/dP=42$ K/GPa. This is ten times the value obtained from ϵ' under pressure (4 K/GPa);[41] the discrepancy may be ascribed to the presence of [110] domains.

Below T_{N1}, ϵ' becomes frequency dependent and shows a broad relaxation peak around 190 K, which is similar to the characteristic behavior of relaxor ferroelectrics.[14,15] In the same temperature region, ΔC_p and α show a broad peak and a shoulderlike feature, respectively. As these anomalies appear immediately below the onset of the sharp transition, the results support the notion[15] that the relaxorlike behavior is triggered by the improper ferroelastic transition. However, the complex manner in which the sharp and broad anomalies are superimposed makes the determination of the order parameters difficult.[14,15]

Although the broad anomalies in ϵ', α, and C_p correspond well with each other, their relation to the ferroelectric soft mode[14,17] with $T_{N2}\approx196$ K is not apparent. If we assume a normal displacive ferroelectric transition at T_{N2}, the frequency dependence of ϵ' may be attributed to the motion of ferroelectric domains.[42] However, such motion does not con-

tribute significantly to entropy, and the origin of the broad thermodynamic anomalies remains unclear. On the other hand, the anomalies in ϵ', α, and C_p can be explained by relaxorlike development of nanoscale cluster polarization[15] but this idea is not consistent with the persistence of the soft mode up to the vicinity of T_{N2}.[14,17] Moreover, while the nanoscale cluster polarization has been speculated in several studies,[15,43] there has been no direct evidence of such entity in $Cd_2Nb_2O_7$.

Still another view is to consider the coupling between the NbO_6 network and the Cd-O′ dipole chains, where each component is mostly responsible for the soft mode and the relaxorlike behavior, respectively.[29,30] In the cubic phase above T_{N1}, there is strong evidence for the dynamic disorder of the Cd ions,[31,44] where these ions hop among equivalent off-center positions. Below the structural transition at T_{N1}, the local environment around the Cd ions becomes less symmetric, facilitating the Cd ions to settle into one of the stable positions.[14,29] Because the distortion at T_{N1} is very small,[18,19] and the local environment is further modified by the ferroelectric distortion of the NbO_6 octahedra, the Cd ions might be expected to order (or freeze) gradually with decreasing temperature.[30] In this view, the frequency dependence of ϵ' is associated with the dynamics of the Cd-O′ dipoles[29,30] and the broad thermal anomalies can be ascribed to the gradual ordering of the Cd ions. It is important to emphasize that the order-disorder and displacive characters of $Cd_2Nb_2O_7$ originate from distinct sublattices: this is different from the well-known perovskites $BaTiO_3$ and $KNbO_3$, in which the BO_6 octahedra are responsible for both the order-disorder and displacive characters of the ferroelectric transitions.[45] For the perovskites, recent studies of x-ray absorption fine structure and nuclear magnetic resonance provided important understanding on the microscopic characters of the ferroelectric transitions.[46] It would be of great interest to perform similar microscopic measurements on $Cd_2Nb_2O_7$ to better understand its complex ferroelectric behavior.

At $T_{N3}=85$ K, the second-order structural transition is accompanied by a sharp peak in ϵ', α, and C_p. Keeping in mind that the magnitude of $\Delta\alpha$ can be affected by the distribution of monoclinic[18] domains below T_{N3}, the application of Ehrenfest relation with $\Delta C_p=0.80$ J K^{-1} mol^{-1} and $\Delta\alpha=-9.0\times10^{-6}$ K^{-1} leads to a large value of $dT_{N3}/dP=-240$ K/GPa. To put this negative value of dT_{N3}/dP into perspective, we recall that the Raman[20,21] and heat-capacity[15] studies found strong resemblance of the behavior to the incommensurate (IC) transitions in the A_2BX_4 systems (where X=halogen or O).[22] For the A_2BX_4 family, Gesi[47] pointed out that strong order-disorder characters are found in systems with a positive dT_{IC}/dP (where T_{IC} is the IC transition temperature), whereas displacive characters are found in systems with a negative dT_{IC}/dP. Interestingly, one of the first hints[20] for the IC character in $Cd_2Nb_2O_7$ came from its strong resemblance of the Raman scattering to K_2SeO_4, which is a prototypical displacive IC system with $dT_{IC}/dP=-65.5$ K/GPa.[22] These considerations suggest a displacive character for the purported IC transition in $Cd_2Nb_2O_7$, although further efforts are certainly needed to find direct evidence of an IC structure. Furthermore, the large negative value of dT_{N3}/dP implies that the coupling of the soft mode to volume strain is appreciable, and it is important to check this point with direct determination of dT_{N3}/dP under pressure.

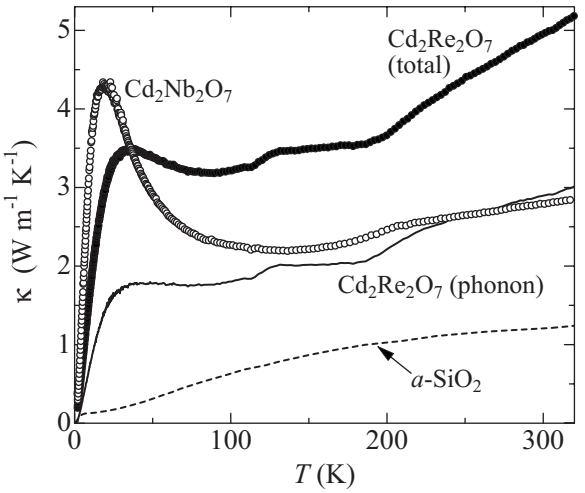

FIG. 6. Thermal conductivity κ of $Cd_2Re_2O_7$ and $Cd_2Nb_2O_7$ measured on heating direction. For $Cd_2Re_2O_7$, the closed circles represent the total κ, whereas the solid line corresponds to the phonon contribution κ_{ph} obtained by subtracting the estimated electronic contribution from the total κ. The κ of amorphous silica a-SiO_2 (Ref. 49) is shown as a dashed line.

At still lower temperature, anomalies in ϵ' and ΔC_p can be found at $T_{N4}=46$ K. The Raman and C_p studies suggested that this is a lock-in transition to a commensurate phase[15,20,21] but no important changes were found at T_{N4} in the structural study.[18] Within the precision of the present measurement, we could not identify any anomaly in $\Delta L/L_0$ or α at this temperature. Considering that the entropy of this transition [0.054 J K^{-1} mol^{-1} (Ref. 15)] is only slightly smaller than that of $Cd_2Re_2O_7$ at T_{R2}, our failure to observe an anomaly in α suggests that dT_{N4}/dP is much smaller than ±26 K/GPa found for dT_{R2}/dP.

C. Thermal conductivity of $Cd_2Re_2O_7$ and $Cd_2Nb_2O_7$

Finally, we discuss the thermal conductivity κ of $Cd_2Re_2O_7$ and $Cd_2Nb_2O_7$, which are shown in Fig. 6. For $Cd_2Re_2O_7$, κ shows a change in slope near T_{R1} and a steplike anomaly at T_{R2}, which reflect changes in the degree of scattering or scattering mechanism for the heat carriers at the structural transitions. These anomalies and the peak at 35 K are more pronounced than those reported in Ref. 28, suggesting higher crystalline quality of the present sample. An estimate for the phonon contribution κ_{ph} can be obtained by subtracting the electronic contribution κ_{el} from the total κ, where κ_{el} is obtained from ρ using the Widemann-Franz law.[48] In Fig. 6, κ_{ph} is plotted as a solid line, which shows that the anomalies around the transitions are mainly associated with phonons. On the other hand, the peak in the total κ at 35 K is almost completely removed in κ_{ph}. For ordinary crystalline materials, κ_{ph} decreases with a $\sim1/T$ dependence above the peak temperature (typically $\sim10-70$ K), due to the decrease in phonon mean-free path from intrinsic phonon-phonon interactions.[48] In contrast, κ_{ph} of $Cd_2Re_2O_7$

is small and almost temperature independent within the tetragonal phases above 50 K, and shows a glasslike $d\kappa_{ph}/dT>0$ behavior in the cubic phase (κ of amorphous silica[49] is shown in Fig. 6). These results indicate the presence of additional phonon scattering mechanisms in $Cd_2Re_2O_7$. In Ref. 28, the $d\kappa_{ph}/dT>0$ behavior was attributed to strong interaction of the heat-carrying acoustic phonons with the localized Einstein oscillation of the Cd ions; evidence for this mechanism was provided by the presence of an Einstein mode in C_p with the characteristic temperature $\Theta_E \approx 98$ K, which matches with the mean-square displacement amplitude of the Cd ions.[28] For the pyrochlore structure, it is possible to consider the small Cd ions[2] as residing in the oversized voids created by the network of BO_6 octahedra,[29] which could result in large dynamic displacement of the Cd ions. Accordingly, the decoupled dynamics of the Cd ions from the main lattice can serve as an extra decay channel for the heat-carrying acoustic phonons. In this view, the anomaly near T_{R1} might be ascribed to a change in the dynamical properties of the Cd ions, although there may be additional contributions from the Goldstone excitations[9,10] (either as a heat carrier or scatterer) below T_{R1}. For the structural transition at T_{R2}, the Raman-scattering study[27] pointed to the ordering of the Cd ions as the driving mechanism of the transition. In this regard, one may expect κ_{ph} to increase below T_{R2}, but the opposite is found in Fig. 6. This suggests that the reduction in κ_{ph} is attributed to increased phonon scattering from the additional optic modes below T_{R2}.[27]

Similar $d\kappa/dT>0$ behavior is found for the cubic phase of $Cd_2Nb_2O_7$ in which heat is transported entirely by phonons. For this compound, the previous C_p study[15] found an Einstein mode with $\Theta_E \approx 76$ K, and large displacement amplitude for the Cd ions has been reported.[44,50] Moreover, the recent diffuse x-ray scattering study provided strong evidence for the dynamic disorder of the Cd ions in the cubic phase,[31] suggesting that the $d\kappa/dT>0$ behavior is associated with strong phonon damping by the Cd ions. It is interesting to note that similar $d\kappa/dT>0$ behavior is found in the KH_2PO_4 family of hydrogen-bond ferroelectrics,[51] where $d\kappa/dT>0$ in the paraelectric phase is ascribed to strong phonon scattering from the disorder in hydrogen positions. However, whereas the hydrogen-bonded systems show a recovery of conventional $d\kappa/dT<0$ behavior upon entering the ordered ferroelectric phase,[51] κ of $Cd_2Nb_2O_7$ is suppressed further below T_{N1}. This suggests the presence of different scattering mechanisms below T_{N1}, and it is tempting to associate it with the relaxorlike behavior in this temperature region. Especially, as the Cd ions order gradually below T_{N1}, local strains are expected to develop and this can be a significant source of phonon scattering. In agreement with this idea, κ starts to show a $1/T$ behavior below ~ 100 K, where the relaxorlike behavior is no longer found in ϵ' and C_p. Within the precision of the present measurement, there is no obvious anomaly at T_{N3} and T_{N4}. The sharp maximum at 18 K signifies the absence of significant disorder in the crystal, suggesting that the Cd ions are fully ordered in the low-temperature regions. This is consistent with the absence of glasslike T-linear term in C_p below 1 K.[15]

IV. SUMMARY

In summary, we have studied the structural phase transitions in $Cd_2Re_2O_7$ and $Cd_2Nb_2O_7$ through measurements of thermal expansion, heat capacity, and thermal conductivity. The use of high-quality single crystals allowed detailed examination of the structural transitions, including the pressure dependence of the transition temperatures through the application of thermodynamic relations. The thermal properties of $Cd_2Nb_2O_7$ show complex behavior, especially near the relaxorlike feature around 190 K. For both compounds, the lattice thermal conductivity has a glasslike temperature dependence in the cubic phase, which can be associated with the unusual dynamics of the Cd ions. Further work is needed to understand the specific roles of the Cd ions in the intriguing structural transitions.

ACKNOWLEDGMENTS

We are grateful to M. Rotter and H. Müller for constructing the dilatometer cell and providing expertise on the measurement technique. We also thank H. S. Suzuki for assistance in aligning the crystals. This study was supported by a Grant-in-Aid from JSPS under Grants No. 20740178 and No. 22246083, and WPI Research Center Initiative on Materials Nanoarchitechtonics from MEXT, Japan.

[1] J. S. Gardner, M. J. P. Gingras, and J. E. Greedan, Rev. Mod. Phys. **82**, 53 (2010).
[2] M. A. Subramanian, G. Aravamudan, and G. V. Subba Rao, Prog. Solid State Chem. **15**, 55 (1983).
[3] A. P. Ramirez and M. A. Subramanian, Science **277**, 546 (1997).
[4] M. Hanawa, Y. Muraoka, T. Tayama, T. Sakakibara, J. Yamaura, and Z. Hiroi, Phys. Rev. Lett. **87**, 187001 (2001).
[5] J. Yamaura and Z. Hiroi, J. Phys. Soc. Jpn. **71**, 2598 (2002).
[6] I. A. Sergienko and S. H. Curnoe, J. Phys. Soc. Jpn. **72**, 1607 (2003).
[7] I. A. Sergienko, V. Keppens, M. McGuire, R. Jin, J. He, S. H. Curnoe, B. C. Sales, P. Blaha, D. J. Singh, K. Schwarz, and D. Mandrus, Phys. Rev. Lett. **92**, 065501 (2004).
[8] Here, the term "ferroelectric" is used in a weaker sense (Ref. 7), as the tetragonal $Cd_2Re_2O_7$ is piezoelectric but not pyroelectric; Y. Ishibashi and M. Iwata, J. Phys. Soc. Jpn. **79**, 044604 (2010).
[9] C. A. Kendziora, I. A. Sergienko, R. Jin, J. He, V. Keppens, B. C. Sales, and D. Mandrus, Phys. Rev. Lett. **95**, 125503 (2005).
[10] J. C. Petersen, M. D. Caswell, J. S. Dodge, I. A. Sergienko, J. He, R. Jin, and D. Mandrus, Nat. Phys. **2**, 605 (2006).
[11] Z. Hiroi, J. Yamaura, Y. Muraoka, and M. Hanawa, J. Phys. Soc. Jpn. **71**, 1634 (2002).
[12] Z. Hiroi, T. Yamauchi, T. Yamada, M. Hanawa, Y. Ohishi, O. Shimomura, M. Abliz, M. Hedo, and Y. Uwatoko, J. Phys. Soc.

Jpn. **71**, 1553 (2002).
[13] N. Barišić, L. Forró, D. Mandrus, R. Jin, J. He, and P. Fazekas, Phys. Rev. B **67**, 245112 (2003).
[14] E. Buixaderas, S. Kamba, J. Petzelt, M. Savinov, and N. N. Kolpakova, Eur. Phys. J. B **19**, 9 (2001).
[15] M. Tachibana, H. Kawaji, and T. Atake, Phys. Rev. B **70**, 064103 (2004).
[16] A. A. Bokov and Z.-G. Ye, J. Mater. Sci. **41**, 31 (2006).
[17] H. Taniguchi, T. Shimizu, H. Kawaji, T. Atake, M. Itoh, and M. Tachibana, Phys. Rev. B **77**, 224104 (2008).
[18] A. Küster, J. Ihringer, W. Limper, T. Wroblewski, and W. Prandl, Mater. Sci. Forum **79-82**, 791 (1991).
[19] M. Fischer, T. Malcherek, U. Bismayer, P. Blaha, and K. Schwarz, Phys. Rev. B **78**, 014108 (2008).
[20] N. N. Kolpakova, B. Březina, and E. S. Sher, Jpn. J. Appl. Phys., Suppl. **24-2**, 823 (1985).
[21] G. A. Smolensky, N. N. Kolpakova, S. A. Kizhaev, and E. S. Sher, Ferroelectrics **73**, 161 (1987).
[22] H. Z. Cummins, Phys. Rep. **185**, 211 (1990).
[23] A structural transition at 200 K in $Cd_2Ta_2O_7$ has been reported in Ref. 24 but this transition is not reproduced in later studies. See, e.g., N. N. Kolpakova, M. Wiesner, G. Kugel, and P. Bourson, Ferroelectrics **201**, 107 (1997).
[24] A. W. Sleight and J. D. Bierlein, Solid State Commun. **18**, 163 (1976).
[25] G. A. Samara, T. Sakudo, and K. Yoshimitsu, Phys. Rev. Lett. **35**, 1767 (1975).
[26] G. A. Samara and P. S. Peercy, in *Solid State Physics*, edited by H. Ehrenreich, F. Seitz, and D. Turnbull (Academic Press, New York, 1981), Vol. 36, p.1.
[27] C. S. Knee, J. Holmlund, J. Andreasson, M. Käll, S. G. Eriksson, and L. Börjesson, Phys. Rev. B **71**, 214518 (2005).
[28] J. He, D. Hitchcock, I. Bredeson, N. Hickman, T. M. Tritt, and S. N. Zhang, Phys. Rev. B **81**, 134302 (2010).
[29] N. N. Kolpakova, S. Waplak, and W. Bednarski, J. Phys.: Condens. Matter **10**, 9309 (1998).
[30] N. N. Kolpakova, P. P. Syrnikov, A. O. Lebedev, P. Czarnecki, W. Nawrocik, C. Perrot, and L. Szczepanska, J. Appl. Phys. **90**, 6332 (2001).
[31] M. Paściak, M. Wołcyrz, A. Pietraszko, and S. Leoni, Phys. Rev. B **81**, 014107 (2010).
[32] M. Tachibana, T. Kolodiazhnyi, and E. Takayama-Muromachi, Appl. Phys. Lett. **93**, 092902 (2008).
[33] M. Rotter, H. Müller, E. Gratz, M. Doerr, and M. Loewenhaupt, Rev. Sci. Instrum. **69**, 2742 (1998).
[34] B. Golding, Phys. Rev. Lett. **25**, 1439 (1970).
[35] R. Jin, J. He, J. R. Thompson, M. F. Chisholm, B. C. Sales, and D. Mandrus, J. Phys.: Condens. Matter **14**, L117 (2002).
[36] J. P. Castellan, B. D. Gaulin, J. van Duijn, M. J. Lewis, M. D. Lumsden, R. Jin, J. He, S. E. Nagler, and D. Mandrus, Phys. Rev. B **66**, 134528 (2002).
[37] M. T. Weller, R. W. Hughes, J. Rooke, C. S. Knee, and J. Reading, Dalton Trans. **19**, 3032 (2004).
[38] Although the Eherenfest relation is based on a mean-field transition, it can be applied to λ-type transitions if the same criterion is used to obtain the jumps in C_p and α, T. Lorenz, H. Kierspel, S. Kleefisch, B. Büchner, E. Gamper, A. Revcolevschi, and G. Dhalenne, Phys. Rev. B **56**, R501 (1997).
[39] P. W. Anderson and E. I. Blount, Phys. Rev. Lett. **14**, 217 (1965).
[40] C. Lu, J. Zhang, R. Jin, H. Qu, J. He, D. Mandrus, K. D. Tsuei, C. T. Tzeng, L. C. Lin, and E. W. Plummer, Phys. Rev. B **70**, 092506 (2004).
[41] N. Yasuda, S. Fujimoto, K. Tanaka, and T. Hachiga, J. Phys. D: Appl. Phys. **17**, 2069 (1984).
[42] C. Ang, R. Guo, A. S. Bhalla, and L. E. Cross, J. Appl. Phys. **87**, 7452 (2000).
[43] C. Ang, L. E. Cross, R. Guo, and A. S. Bhalla, Appl. Phys. Lett. **77**, 732 (2000).
[44] K. Lukaszewicz, A. Pietraszko, J. Stepien-Damm, and N. N. Kolpakova, Mater. Res. Bull. **29**, 987 (1994).
[45] T. P. Dougherty, G. P. Wiederrecht, K. A. Nelson, M. H. Garrett, H. P. Jensen, and C. Warde, Science **258**, 770 (1992).
[46] E. A. Stern, Phys. Rev. Lett. **93**, 037601 (2004).
[47] K. Gesi, J. Phys. Soc. Jpn. **59**, 1841 (1990).
[48] R. Berman, *Thermal Conduction in Solids* (Oxford University Press, Oxford, 1976).
[49] D. G. Cahill, S. K. Watson, and R. O. Pohl, Phys. Rev. B **46**, 6131 (1992).
[50] T. Malcherek, U. Bismayer, and C. Paulmann, J. Phys.: Condens. Matter **22**, 205401 (2010).
[51] Y. Suemune, J. Phys. Soc. Jpn. **22**, 735 (1967).